High-Pressure NMR of Polymers Dissolved in Supercritical Carbon Dioxide

Alexander Dardin, J. B. Cain, J. M. DeSimone,* C. S. Johnson, Jr., and E. T. Samulski*

CB#3290 Venable and Kenan Laboratories, Department of Chemistry, University of North Carolina at Chapel Hill, Chapel Hill, North Carolina, 27599-3290

Received December 27, 1996; Revised Manuscript Received March 20, 1997[⊗]

ABSTRACT: High-pressure, high-resolution proton nuclear magnetic resonance spectroscopy has been utilized to study the solution behavior of poly(1,1-dihydroperfluorooctyl acrylate) (PFOA) and poly(1,1-dihydroperfluorooctyl acrylate-*block*-styrene) (PFOA-*b*-PS) in supercritical carbon dioxide. The proton chemical shift was monitored as a function of solvent density and temperature. A change in the solvent quality of CO_2 from that of a poor solvent to that of a good solvent is postulated to describe a discontinuous change in the ^{1}H NMR spectra of the polymers with increasing CO_2 density and increasing temperature. At a CO_2 density of 0.7 g cm^{-3} at 64.6 °C (0.8 g cm^{-3} at 41.2 °C) there is an apparent transition between a two-phase system—the coexistence of two polymer species in different environments—and a homogeneous solution. The volume fraction of CO_2 in the polymer-rich phase is estimated from the proton chemical shift and the contributions from the bulk susceptibilities of PFOA and PFOA-*b*-PS.

Introduction

While liquid carbon dioxide and supercritical carbon dioxide are already well established as an extraction medium[1,2] only in the last few years CO_2 has been shown to be a powerful solvent for organic reactions and polymerizations.[3−8] CO_2's ability to plasticize many polymers[9] and even dissolve fluorinated polymers make CO_2 a potentially important substitute for environmentally harmful chlorofluorocarbons (CFC's) and other organic solvents for polymer synthesis and processing.[1] Furthermore, it is possible to tune many of the properties of CO_2 (e.g. density, dielectric constant and solubility parameter), i.e., to adjust the solvent quality, through temperature and pressure profiling (Figure 1).

Although many different low molar mass compounds are soluble in CO_2,[1,10] only very few polymeric materials (amorphous fluoropolymers and silicones) are known to be readily soluble in CO_2 under reasonably accessible conditions (T < 100 °C; P < 300 bar).[1,3,11] Some of these "CO_2-philic" materials can be homogeneously synthesized in liquid and supercritical CO_2.[4] Moreover, CO_2-soluble polymers and CO_2-soluble block copolymers also play an important role as steric stabilizers in dispersion polymerizations of methyl methacrylate or styrene in CO_2.[6,7,12,13] This potential for significant manufacturing applications prompts us to examine more carefully the nature of macromolecular solubility in CO_2.

The solution behavior of CO_2-soluble polymers and micelle-forming block copolymers has already been investigated by X-ray[14] and small angle neutron scattering,[15,16] techniques that give information about the size and shape of these macromolecules (and their aggregates) and the second virial coefficients, A_2, i.e. the interactions between polymer segments and solvent. On the other hand, the plasticization of CO_2-insoluble polymers by CO_2 has been studied by means of UV, FT-IR, and solid state NMR spectroscopy.[17,18] High-pressure, high-resolution nuclear magnetic resonance (HPHR-NMR) spectroscopy has been successfully used to study solubility, media effects, van der Waals interactions, and solute−solvent interactions exhibited by small organic molecules dissolved in liquid or supercritical CO_2.[19−21] However, NMR investigations of macromolecules dissolved in CO_2 have not yet been reported. Herein, we demonstrate the use of proton HPHR-NMR to study the influence of CO_2 density on the solution behavior of poly(1,1-dihydroperfluorooctyl acrylate) (PFOA) and poly(1,1-dihydroperfluorooctyl acrylate-*block*-styrene) (PFOA-*b*-PS) in supercritical carbon dioxide.

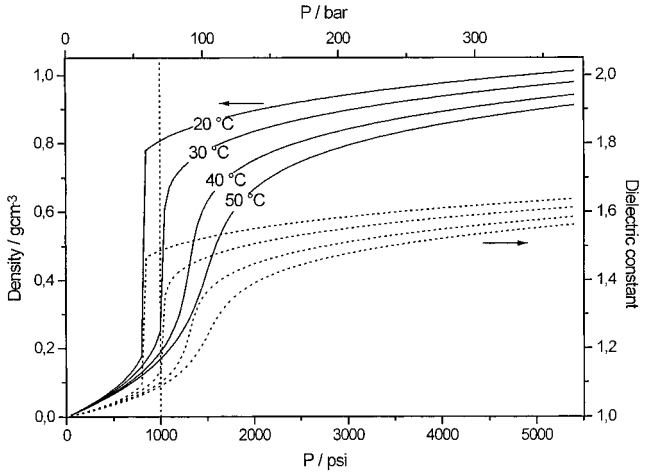

Figure 1. Density (solid line) and dielectric constant (dotted line) of CO_2 as a function of pressure and temperature. The vertical line represents the critical pressure of CO_2 at 1030 psi (71 bar).

Experimental Section

PFOA was synthesized by using homogeneous free radical polymerization methods in CO_2 with AIBN as initiator as described elsewhere.[22] The weight average molecular weight, M_w, was estimated from neutron scattering experiments to be about 1.33×10^5 and visible cloudpoints were determined for various concentrations and temperatures.[23] The ^{1}H NMR spectrum of PFOA dissolved in a mixture of Freon-113 and $CDCl_3$ consists of five characteristic, broad peaks at 4.65 ppm (side chain, −O−CH_2−), 2.6 ppm (backbone, ⟩CH−), and 2.15, 1.85, and 1.69 ppm (backbone, −CH_2−), respectively. The corresponding hydrogenated monomer 1,1-dihydroperfluorooctyl propionate (HFOA) has been prepared by standard heterogeneous hydrogenation methods using a Wilkinson catalyst.[24]

* Authors to whom correspondence should be addressed.
[⊗] Abstract published in *Advance ACS Abstracts,* May 1, 1997.

S0024-9297(96)01917-1 CCC: $14.00

PFOA-*b*-PS was prepared by the iniferter method using tetraethylthiuram disulfide as described earlier.[25] The average molecular weight of the polystyrene macroinitiator was determined to be 6.6×10^3 by gel permeation chromatography (GPC), the molecular weight of the PFOA block was obtained from ^{1}H NMR ($M_n = 3.5 \times 10^4$). In addition to the resonances of PFOA, PFOA-*b*-PS shows the aromatic ^{1}H signals of polystyrene between 6 and 8 ppm.

High-Pressure ^{1}H NMR Experiments. High-resolution ^{1}H NMR spectra were recorded on a Bruker MSL-360 spectrometer operating at a proton frequency of 360.13 MHz (8.455 T). The length of the 90° pulse was 4.95 μs and the recycle delay was set to 5 s ($>5T_1$) for all experiments.

The high pressure setup utilized herein was based on the cell design of Yonker *et al.*[26,27] which was interfaced with our standard high-pressure equipment. The high-pressure NMR cell consists of a polyimide-coated glass capillary (Polymicro Tech.) with an inner diameter of 150 μm. The capillary was folded repeatedly (21 times with a fold length of 5 cm) and fits into a regular 5 mm NMR tube which in turn was attached to a 70 cm glass tube conduit for the capillary out of the top opening of the magnet. One end of the capillary was connected to a custom made, 2.5 mL stainless steel high-pressure view cell interfaced with a pressure generator pump using standard high-pressure valves and tubing (High Pressure Equipment, HIP); the other end was sealed with a high-pressure valve. The total volume of this setup including view cell, valves, and tubing was measured to be 6.4 mL.

The volume surrounding the capillary in the NMR tube was filled with $CDCl_3$, which was used as an external lock solvent and also served as an external reference for the determination of chemical shifts. The temperature in the observation region of the capillary was controlled by the Bruker VT-1000 unit which was calibrated against an external thermocouple and was constant within ±1 K. Pressure up to 350 bar was applied by a hand-driven pressure generator (HIP) and measured with a calibrated transducer (Sensotec).

Prior to recording the NMR spectra, 0.125 g of the sample was first placed in the high-pressure view cell and pressurized with CO_2 (Air Products) to 300 bar. The mixture was stirred with a magnetic stir bar and within 10 min a clear 2 w/vol % solution was obtained. The solution was kept under pressure overnight to ensure complete dissolution of the polymer. After the external setup was connected to the capillary, the polymer solution was allowed to flow into the capillary. Air initially in the capillary was flushed out by opening the valve at the end of the capillary. The volume of the capillary tubing is essentially negligible relative to the volume of the high-pressure setup, resulting in only a short and small pressure drop during this process. Then, the pressure of the system and the temperature in the NMR probe were set to the desired value and checked to be stable over the period of 1 h.

Pressure-dependent NMR experiments were carried out starting at low CO_2 densities, i.e. a pressure of about 100 bar at temperatures of 41.2 and 64.6 °C, respectively. After each incremental pressure increase of about 10 to 25 bar, the system was allowed to equilibrate until the pressure reading was stable for at least 20 min. The pressure in the system was then constant within ±0.345 bar (±5 psi on the instrument).

Background

In general, the chemical shift of a substance dissolved in a solvent is dominated by the volume (bulk) magnetic susceptibility χ_v of the medium. The effective magnetic field strength, H_{eff}, in a cylindrical sample parallel to the magnetic field is then given by (cgs units)[28]

$$H_{eff} = (1 - \sigma_b)H_o = H_o\left[1 + \frac{4\pi}{3}\chi_v\right] \qquad (1)$$

where H_o is the externally applied magnetic field strength. This relationship in turn gives the expression for the screening constant, σ_b, due to the bulk susceptibility:

$$\sigma_b = -\frac{4\pi}{3}\chi_v = -\frac{4\pi\chi_m}{3V_m} = -\frac{4\pi\chi_m}{3M}\rho \qquad (2)$$

where χ_m is the molar susceptibility, V_m the molar volume, M the molecular weight, and ρ the density of the medium.

In order to investigate medium effects on the chemical shift of a solute, one may use a virial expansion of the shielding constant σ in powers of the reciprocal molar volume V_m of the medium:[29]

$$\sigma = \sigma_o + \frac{\sigma_1}{V_m} + \frac{\sigma_2}{V_m^2} + \ldots \qquad (3)$$

Here σ_o is the corresponding shielding of the solute in vacuo and σ_1 is the second virial coefficient of the shielding resulting from binary collisions, while σ_2, σ_3, ... correspond to ternary and higher order contributions. Usually all of these higher order terms except the binary collisions can be neglected. σ_1 generally contains contributions from the bulk susceptibility σ_b (see eq 2), the van der Waals interactions (σ_w), a term arising from dipolar interactions in polar solvents, σ_E, and a contribution from the anisotropy of the molecular susceptibility, σ_a:[30]

$$\sigma_1 = \sigma_b + \sigma_w + \sigma_E + \sigma_a \qquad (4)$$

Ignoring anisotropic and specific solvent-solute contributions (i.e., $\sigma_1 \approx \sigma_b$), eqs 2−4 can be written as

$$\sigma = \sigma_0 - \frac{4\pi}{3}\chi_v = \sigma_0 - \frac{4\pi\chi_m}{3Mn}\rho \qquad (5)$$

The validity of eq 5 for the experimental setup used in the investigation presented here was verified by recording ^{13}C NMR spectra of pure CO_2 at 64.6 °C and various pressures in the capillary cell. From the plot of the ^{13}C chemical shift vs CO_2 density a slope of -2.015×10^{-6} cm^3 g^{-1} was obtained. This corresponds to a volume magnetic susceptibility for CO_2 of -0.841×10^{-6}, which is in good agreement with the value of -0.473×10^{-6} reported in the literature.[31]

For a solution, i.e. a mixture of a solute in a solvent, the total bulk susceptibility of the medium has to be taken into account. In a two-component one-phase system, the total volume magnetic susceptibility, χ_v^{tot}, is given by the sum of the single component contributions, χ_v^i, weighted by their volume fractions ϕ_v^i (Wiedemann's additivity law[32]):

$$\chi_v^{tot} = \phi_v^1\chi_v^1 + \phi_v^2\chi_v^2 \qquad (6)$$

Table 1 summarizes the susceptibility and chemical shift data used for the calculations in our study. The chemical shift of the pure polymer and the corresponding value for σ_0 have been assumed to be identical with the monomeric unit (HFOA). The bulk susceptibility of HFOA has been determined using the method of Frei *et al.*[33]

Results and Discussion

Phase Behavior of PFOA. Figure 2 shows the high-resolution ^{1}H NMR spectra of PFOA in supercritical CO_2 which were recorded at increasing CO_2 pressures from 100.6 to 341.2 bar while the temperature was kept constant at 64.6 °C. Under these conditions, the cor-

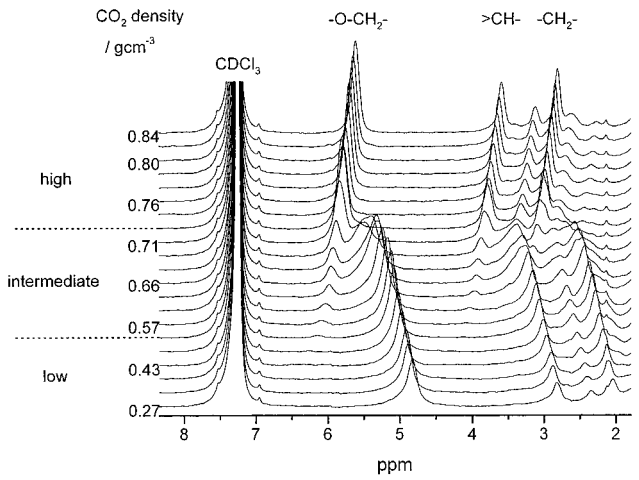

Figure 2. Experimental high-pressure ^{1}H NMR spectra of PFOA in CO_2 at T = 337.8 K (64.6 °C) and CO_2 densities between 0.27 g cm^{-3} (bottom trace) and 0.84 g cm^{-3} (top trace). The spectra were recorded with 256 signal accumulations and a recycle delay of 5 s. Prior to the Fourier transformation, an exponential line broadening of 5 Hz was applied.

Table 1. Data Used for the Calculation

	ρ/g cm^{-3}	σ_0/ppm	σ_p/ppm	χ_v(lit.)/10^{-6}	χ_v(expt)/10^{-6}
CO_2	variable			−0.473[31]	−0.481[a]
PFOA	1.63[b]	7.18	4.62		−0.386[c]

[a] Determined for CO_2 in the capillary setup. [b] Values have been measured for the hydrogenated monomer (HFOA). [c] According to the method of Frei.[33]

responding CO_2 density[34] was varied from 0.27 up to 0.84 g cm^{-3}. All of the characteristic ^{1}H resonances of PFOA observed in a mixture of Freon/$CDCl_3$ can also be found in the spectra recorded under the high pressure conditions, although at different chemical shifts; the line widths are comparable in both solvents. It should be noted that at constant CO_2 pressure/density and temperature no changes in the position of the resonances were observed over a period of 24 h.

In Figure 2 there appear to be three distinct density regions (labeled low, intermediate, and high) where characteristic spectra are obtained. Incrementally increasing the CO_2 density from 0.27 to 0.584 g cm^{-3} (low density regime) results in a monotonic shift of all the PFOA resonances to lower magnetic field strength. However, above a solvent density of 0.584 g cm^{-3}, a second distinct set of PFOA resonances appears which is positioned at ∼1 ppm to lower field. This shift to lower field is readily apparent in the isolated −O−CH_2− resonances at 5.2 and 6.1 ppm, respectively. In the density region between 0.584 and 0.707 g cm^{-3} (intermediate density regime), two spearate PFOA spectra are superposed indicative of a coexistence region—two species of PFOA macromolecules existing in two apparently different environments. In the following discussion, we assign the PFOA spectrum in the low density regime to species **I** and that in the intermediate density to species **II**. In contrast with the resonances of PFOA species **I** (which continue to shift to lower field with increasing density) the resonances of the new PFOA species **II** steadily shift to higher field. For CO_2 densities higher than 0.707 g cm^{-3}, the resonances of species **I** disappear and only the species **II** PFOA resonances are observed. This divergence in chemical shifts of species **I** and **II** with increasing solvent density is illustrated for the methoxy resonances in Figure 3 at two different temperatures. All signals of PFOA, i.e.

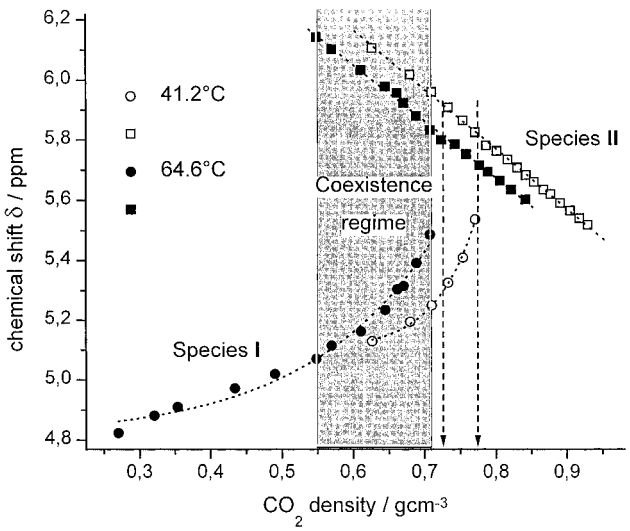

Figure 3. ^{1}H chemical shift of PFOA (−O−CH_2− resonances) as a function of CO_2 density for T = 314.35 K (41.2 °C) (open symbols) and T = 337.75 K (64.6 °C) (closed symbols). The two arrows indicate the cloudpoints found at these temperatures. For the data recorded at T = 337.75 K, the coexistence region is shown in the shaded box.

the resonances of the protons along the polymer backbone in the region between 2 and 4 ppm, show the same absolute change in chemical shift with increasing density. In the remaining discussions, we focus on the better resolved −O−CH_2− signals.

For a homogeneous solution of PFOA dissolved in CO_2, a linear relationship between the chemical shift of the solute and the total density of the medium can be expected according to eq 5. For the very low polymer concentration of about 2 w/vol % used in these investigations, we assume that according to eq 6 the contributions of the polymer to the total bulk susceptibility of the solution are negligible. In the absence of specific solvent−solute interactions, the slope of the plot of the chemical shift vs density according to eq 2 should give the bulk susceptibility of CO_2, -1.98×10^{-6} cm^3 g^{-1}. At both high temperatures in Figure 3, the chemical shift of the PFOA species **II** in the intermediate and high density regimes exhibits the expected linear behavior giving slopes of -1.97×10^{-6} cm^3 g^{-1} at 41.2 °C and -1.89×10^{-6} cm^3 g^{-1} at 64.6 °C, respectively. Deviations from the theoretical value (-1.98×10^{-6} cm^3 g^{-1}) can be attributed to a contribution from the solubilized polymer to the total density and bulk susceptibility. Also imperfect parallel alignment of the capillary in the magnetic field may contribute to the observed values of σ. In agreement with recent *ab initio* calculations reported by Cece *et al.*,[35] our findings support the suggestion that no or only minor specific interactions between CO_2 and C−H bonds contribute to the proton's screening constant. Nevertheless, even without specific interactions, the chemical shift data of PFOA species **II** in CO_2 in the intermediate and high density regimes are indicative of well-dissolved polymers.

This is not the case for species **I**. According to the ^{1}H resonances of PFOA species **I** in the intermediate density regime, its chemical shifts are very close to those of species **II**. According to Figure 3, the −O−CH_2 resonances asymptotically approach a value of about 4.8 ppm with decreasing density in the low density region. We estimate the chemical shift of the −O−CH_2− unit to be 4.62 ppm in the bulk polymer, i.e. in the absence

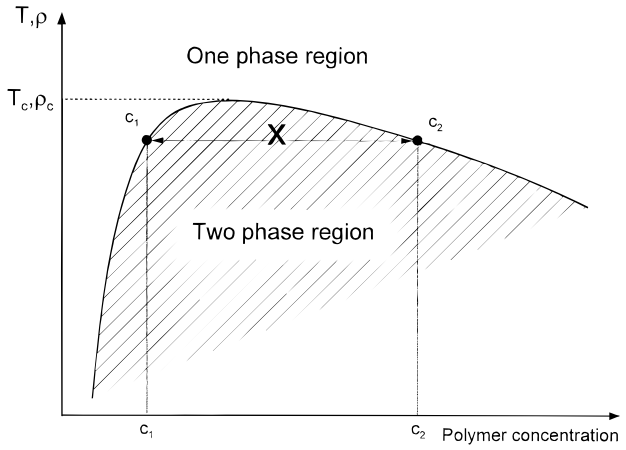

Figure 4. Schematic phase diagram of a polymer solution with an upper critical solution temperature (UCST). A polymer solution of initial polymer concentration x phase-separates below T_c into a polymer-poor phase with concentration c_1 and a polymer-rich phase (c_2).

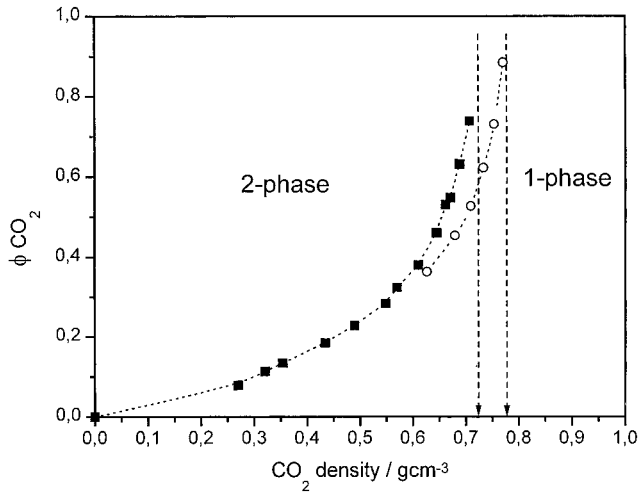

Figure 5. Volume fraction of CO_2 in the polymer-rich phase at $T = 314.35$ K (41.2 °C) (○) and $T = 337.75$ K (64.6 °C) (■). The vertical arrows indicate the optical cloudpoints observed at these temperatures.

of any solvent, from the spectrum of the pure hydrogenated monomer HFOA (taken in a single capillary surrounded by $CDCl_3$). We conclude therefore that the PFOA species **I** in the low and intermediate density regime exists in an CO_2-depleted environment relative to species **II**. With decreasing CO_2 density the environment increasingly excludes solvent, eventually approaching the state of a pure, unswollen polymer phase. Thus, the observation of two different polymer environments—one where the polymer is well dissolved in CO_2 (species **II**) and one where little CO_2 is present (species **I**)—as well as a coexistence regime of both polymer species suggests that the transition from **I** → **II** corresponds to a change in the solvation of PFOA, i.e. a change in the solvent quality of CO_2 for PFOA.

In analogy to polymer solutions showing lower and/or upper critical solution temperatures, we propose the existence of an upper critical solution density (UCSD) for the PFOA/CO_2 system below which the polymer solution separates into a polymer-rich and a polymer-poor phase. NMR studies on critical binary mixtures have shown that two NMR signals of the same molecule simultaneously may be observed when the system phase separates.[36] The suggestion that a similar phase separation occurs in the PFOA/CO_2 system is consonant with cloudpoint measurements.[23] The visible cloudpoints coincide with the transition from the homogeneous phase to the coexistence regime (indicated in Figure 3 by the arrows at 0.724 g cm^{-3} at $T = 64.6$ °C and 0.772 g cm^{-3} at $T = 41.2$ °C, respectively). Recent SANS experiments[15] also support our UCSD hypothesis; the SANS data show that high molecular weight PFOA ($M_w = 1.4 \times 10^6$ g mol^{-1}) passes through a θ-point—an enthalpy driven transition wherein the solvated polymer random coil conformation collapses to a globular conformation and concomitantly excludes solvent from its domain[37,38]—with decreasing pressure at 295 bar and 65 °C ($\rho^{CO_2} = 0.806$ g cm^{-3}). Thus, changing the solvent quality of CO_2 from that of a good solvent for PFOA (positive second virial coefficient A_2) to that of a poor one (negative A_2) results in the formation of a two-phase system. Consequently, we would expect PFOA to exhibit the phase diagram shown schematically in Figure 4. This type of behavior has been observed for many other polymer solutions, e.g. polystyrene in cyclohexane.[39] The only difference here is that PFOA/CO_2 possesses a temperature-dependent θ-*density*.

In the polymer-rich phase PFOA contributes significantly to the total bulk susceptibility of that phase. Accordingly, one can calculate the volume fraction of CO_2, $\phi_v^{CO_2}$, in that phase from the chemical shift of PFOA species **I** with the susceptibility by combining eqs 5 and 6

$$\phi_v^{CO_2} = \left[\frac{3}{4\pi}(\sigma - \sigma_0) - \frac{\chi_m^{PFOA}}{M_n^{PFOA}}\rho^{PFOA}\right] \Bigg/ \left[\frac{\chi_m^{CO_2}}{M_n^{CO_2}}\rho^{CO_2} - \frac{\chi_m^{PFOA}}{M_n^{PFOA}}\rho^{PFOA}\right] \quad (7)$$

In Figure 5 the calculated volume fraction of CO_2 in the polymer-rich phase using the values given in Table 1 is displayed as a function of the CO_2 density for 41.2 and 64.6 °C, respectively. This plot resembles a phase diagram for PFOA in CO_2 having upper critical solution densities (vertical cloud point lines). Reasonable values are obtained for $\phi_v^{CO_2}$ (between 0.08 and 0.88) delineating the side of the composition of the polymer-rich phase of the phase diagram of PFOA in CO_2. At a density of 0.7 g cm^{-3} at 41.2 °C (0.65 g cm^{-3} at 64.6 °C) the volume fraction of CO_2 is already reduced to 0.5 while at lower densities the PFOA-rich phase is rapidly excluding CO_2 and PFOA can be considered to be in a swollen state rather than dissolved. Remarkably, even at only 8 vol % CO_2, PFOA is still sufficiently plasticized to exhibit a resolved NMR spectrum under high-resolution conditions. The swollen PFOA can be considered to be highly mobile with correlation times of segmental mobility much smaller than 10^{-6} s.

From the chemical shift data of PFOA **II** the composition of the polymer-poor phase as well as that of the homogeneous phase should be accessible. However, the chemical shift of PFOA species **II** does not show any significant change at the transition into the two-phase region, indicating that the change in volume fraction of CO_2 is rather small. At very low densities the signal intensity of PFOA species **II** finally disappears. Thus, the volume fraction of PFOA in this phase either is zero or is too small to be detected by NMR.

The molar susceptibility χ_m is in general temperature independent,[32] and therefore no significant changes in the chemical shift are expected with temperature.

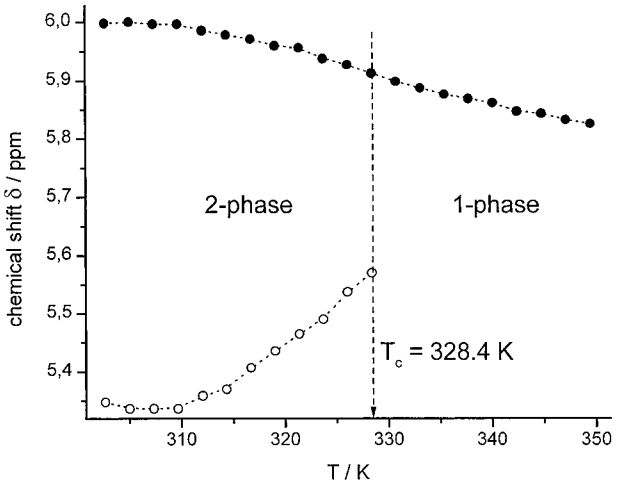

Figure 6. Temperature dependence of the PFOA proton chemical shift (−O−CH_2− resonances) at constant CO_2 density (ρ = 0.733 g cm^{-3}): (○) species **I**; (●) species **II**.

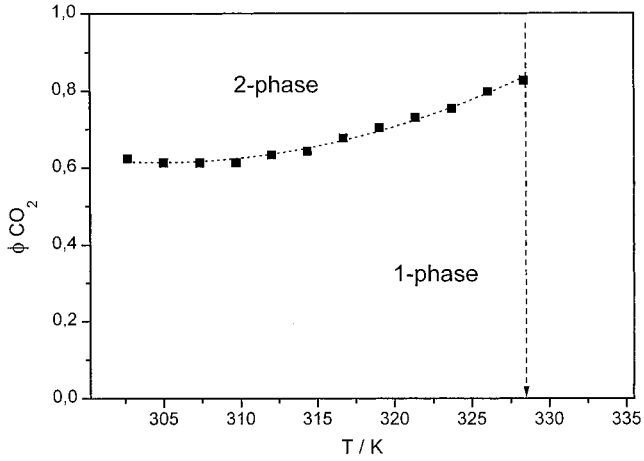

Figure 7. Volume fraction of CO_2 in the polymer-rich phase vs temperature at constant density (0.733 g cm^{-3}). The arrow indicates the critical temperature of the polymer solution.

However, from the chemical shift data in Figure 3 it is obvious that the PFOA resonances exhibit a pronounced temperature dependence at constant density. To study the particular influence of temperature on the solution behavior of PFOA in CO_2, NMR spectra were recorded with increasing temperatures at constant CO_2 density. A density of 0.733 g cm^{-3} was chosen, and the temperature was varied from 29.5 to 76.2 °C, starting the experiments in the two-phase regime of the solution. After each temperature increase, the pressure was readjusted to give an average density of (0.733 ± 6) × 10^{-4} g cm^{-3} for all experiments. The proton chemical shift of the PFOA methoxy group is shown in Figure 6 as a function of temperature. Analogous to the solution behavior at increasing CO_2 density, the PFOA solution is passing an upper critical point (UCST) and showing a transition from a two-phase into a one-phase system. The calculated volume fraction of CO_2, $\phi_v^{CO_2}$, from constant CO_2 density is plotted in Figure 7 against temperature. At this rather high CO_2 density, the phase diagram shows only a narrow two-phase regime with $0.6 < \phi_v < 1$. From these experiments it can be concluded that CO_2 is quite a variable solvent for PFOA. Depending on the temperature, at low CO_2 densities CO_2 is a poor solvent and PFOA coexists in a two-phase system as shown in Figure 4. Increasing solvent density and/or temperature improves the solvent quality of CO_2 significantly, eventually converting CO_2 into a good solvent for PFOA (single-phase solution).

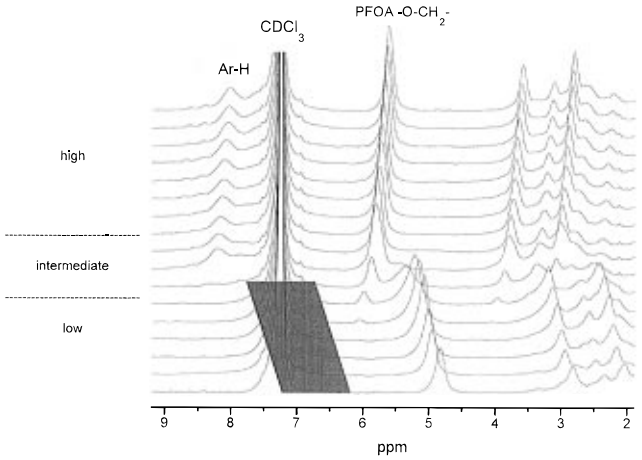

Figure 8. Experimental high-pressure ^{1}H NMR spectra of PFOA-*b*-PS in CO_2 at T = 337.8 K (64.6 °C) and CO_2 densities between 0.26 g cm^{-3} (bottom trace) and 0.85 g cm^{-3} (top trace). The spectra were recorded with 256 signal accumulations and a recycle delay of 5 s. Prior to the Fourier transformation, an exponential line broadening of 5 Hz was applied. The shaded field indicates the region where signals from the PS block are expected for the spectra taken at low densities.

Phase Behavior of the PFOA-*b*-PS Block Copolymer. In this section we will extend our interpretations of PFOA to describe the phase behavior of an amphiphilic block copolymer in CO_2 as determined from HPHR NMR experiments. In analogy to the usual hydrophilic−hydrophobic surfactants, amphiphilic block copolymers comprising a "CO_2-philic" and a "CO_2-phobic" part, for example PFOA-*b*-PS with the polystyrene block being an otherwise completely insoluble "CO_2-phobic" site, have been shown to form micelles in carbon dioxide.[12,15,16] In Figure 8 the HPHR ^{1}H NMR spectra of PFOA-*b*-PS are shown recorded at a temperature of 64.6 °C and CO_2 densities between 0.26 and 0.85 g cm^{-3}.

At low CO_2 densities up to 0.69 g cm^{-3}, only the resonances from the "CO_2-philic" PFOA block are detectable by NMR. Although a part of the chemical shift region where the signal from the aromatic PS protons would be expected (see shaded area in Figure 8) is dominated by the chloroform signal, there is no clear indication of any PS peaks in that area. With increasing solvent density, the PFOA spectrum is first shifted downfield and then passes through the same kind of transition observed for the PFOA homopolymer (see Figure 2). Applying our previous interpretation, at this transition the solvent quality of CO_2 for the PFOA block increases and PFOA changes from a collapsed coil in a polymer-rich phase (species **I**) to a well-dissolved polymer chain in a good solvent (species **II**). Although a significant decrease of the glass transition temperature of plasticized PS under these conditions has been observed in mechanical experiments[40] (i.e., at low frequencies of ∼1 Hz), the aromatic signals for polystyrene remain unobserved up to the end of the coexistence regime at high density. This indicates that polystyrene is completely immobilized on the NMR time scale (10^6 Hz). Thus, the polystyrene block must be located in the micelle core, where it is neither solubilized nor plasticized by CO_2; i.e., PS is immobile by high-resolution NMR criteria up to densities of 0.72 g cm^{-3} at 64.6 °C.

Similar to the PFOA homopolymer, at densities higher than a certain critical density where the coexist-

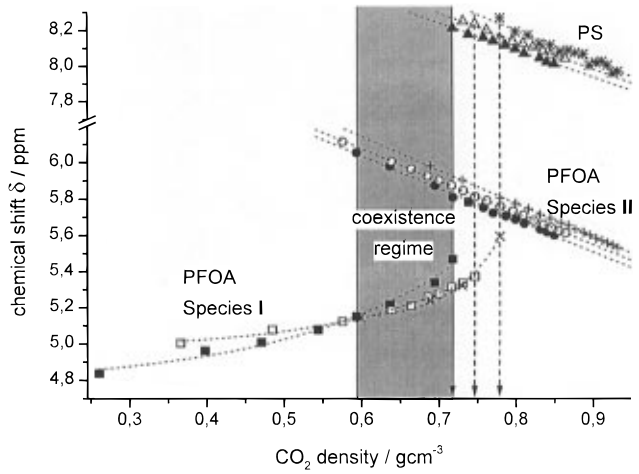

Figure 9. ^{1}H chemical shift of PFOA-*b*-PS ($-O-CH_2-$ and aromatic resonances) as a function of CO_2 density for T = 314.35 K (crosses and stars), T = 327.05 K (open symbols) and T = 337.75 K (full symbols). The arrows indicate the transition densities. For the data recorded at T = 337.75 K, the coexistence region is shown in the shaded box.

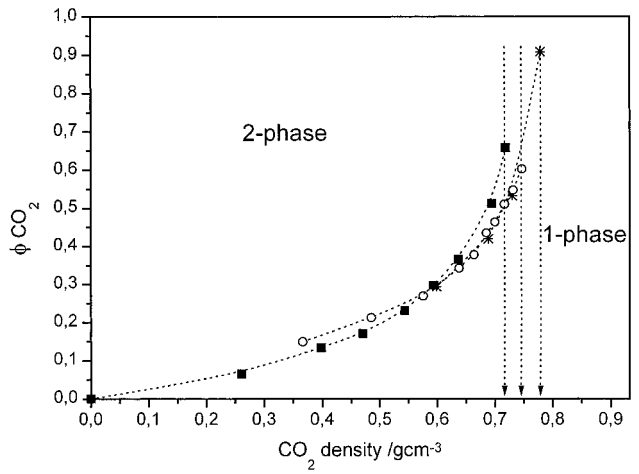

Figure 10. Volume fraction of CO_2 in the polymer-rich phase of the PFOA-*b*-PS solution at T = 314.35 K (*), T = 327.05 K (○), and T = 337.75 K (■). The arrows indicate the critical densities.

ence regime ends, the chemical shift of the PFOA resonances in PFOA-*b*-PS show an upfield shift with increasing CO_2 density. At the same time, NMR signals from the PS block at about 7.5 ppm become visible and also shift upfield. The chemical shifts of PFOA-*b*-PS (the $-O-CH_2-$ resonance of PFOA and the aromatic region of PS are chosen to represent the change in chemical shift of the PFOA and PS block, respectively) are plotted in Figure 9 vs the CO_2 density.

Although PFOA is present only as a part of the PFOA-*b*-PS block copolymer, its chemical shift shows the same behavior as the PFOA homopolymer with increasing solvent density. At low densities the $-O-CH_2-$ resonance is close to the value expected for the pure, i.e. undissolved, polymer (see Table 1). With increasing density of CO_2, a second set of PFOA resonances appears, showing a linear shift to higher field. Again, this second species coexists with the initial one up to a critical density where the polymer solution enters the one-phase regime. According to eq 7, we obtain the volume fractions of CO_2 in the polymer-rich phase from the chemical shifts of species **I** shown in Figure 10.

As soon as the upper critical solution density is reached, NMR signals from the polystyrene block become detectable and also shift upfield with increasing density. The intensity of the PS signal at a CO_2 density of 0.85 g cm^{-3} corresponds to only about 35% of the total aromatic protons. From these findings, we conclude that, above the critical density, parts of the PS block in the micelle core become solubilized in CO_2. This conclusion is reinforced by the linear relationship between the polystyrene signals and the CO_2 density: the chemical shift of the observed styrene units is exclusively influenced by the CO_2 bulk susceptibility. Therefore we anticipate these styrene units to be dissolved in CO_2. Since only 35% of the PS is visible, the entire micelle core is not uniformly plasticized. Instead, the picture that emerges is one where units close to the micelle's core−shell interface are highly mobilized (Figure 11).

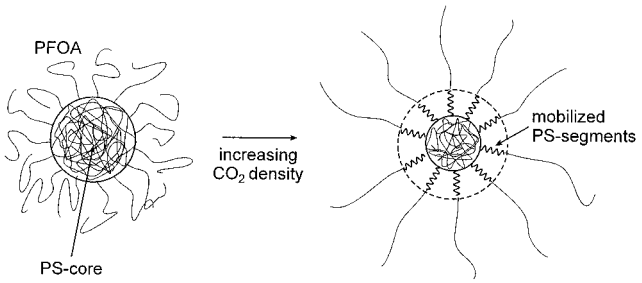

Figure 11. Schematic representation of the solubilization of the PFOA-*b*-PS block copolymer in supercritical CO_2. After the CO_2 density was increased above the critical value, PS units at the core−shell interphase become mobilized.

From the SANS experiments a core diameter of 49 Å was determined for the identical PFOA-*b*-PS block copolymer studied here. Thus, a thin "interphase" shell of less than 7 Å corresponding to two to three styrene units per chain is mobilized when CO_2 becomes a good solvent for the "CO_2-philic" PFOA block.

Concluding Remarks

High-pressure high-resolution NMR spectroscopy has been shown to be a useful technique to study the solution behavior of polymers in supercritical CO_2. Critical parameters such as the upper critical solution temperature (UCST) and an upper critical solution density (UCSD) manifest themselves as a discontinuous change in the proton chemical shift. Below the UCSD and UCST, respectively, CO_2 changes its solvent quality, and the polymer solution crosses a θ-point from a two-phase into a one-phase system.

Furthermore, the chemical shift of the polymer-rich phase can be used to estimate the amount of CO_2 in that phase, thus giving access to an important parameter for the processibility of polymers in CO_2. In the case of block copolymers, NMR gives unique insight into the interphase region of core−shell type supramolecular structures.

Acknowledgment. This research is supported through a research fellowship from the Deutsche Forschungs-gemeinschaft (A.D.) and a grant from the Consortium for Polymeric Materials and Processing in Carbon Dioxide at the University of North Carolina at Chapel Hill, sponsored by Air Products and Chemicals, Bayer, B. F. Goodrich, DuPont, Eastman Chemicals, General Electric, Hoechst-Celanese, and Xerox. J.B.C. and C.S.J. are supported by the ACS-PRF Grant No. 29676-AC7. A.D. thanks Dr. C. D. Poon for his help running the spectrometer and Dr. M. Rubinstein and Dr. A. Dobrynin (University of North Carolina) for many helpful discussions.

References and Notes

(1) McHugh, M. A.; Krukonis, V. J. *Supercritical Fluid Extraction-Principles and Practice*; Butterworth-Heinemann: Woburn, MA, 1994.
(2) Johnston, K. P.; Penninger, J. M. L. *Supercritical Fluid Science and Technology*, ACS Symposium Series 406; American Chemical Society: Washington, DC, 1989.
(3) Hyatt, J. A. *J. Org. Chem.* **1984**, *49*, 5097.
(4) DeSimone, J. M.; Guan, Z.; Elsbernd, C. S. *Science* **1992**, *257*, 954.
(5) DeSimone, J. M.; Shaffer, K. A. *Trends Polym. Sci.* **1995**, *3*, 146.
(6) DeSimone, J. M.; Maury, E. E.; Menceloglu, Y. Z.; Combes, J. R.; McClain, J. B.; Romack, T. J. *Science* **1994**, *265*, 356.
(7) Cooper, A. I.; DeSimone, J. M. *Curr. Opin. Solid State Mater. Sci.* **1996**, *1*, 761.
(8) Canelas, D. A.; Betts, D. E.; DeSimone, J. M. *Macromolecules* **1996**, *29*, 2818.
(9) Wissinger, R. G.; Paulaitis, M. E. *J. Polym. Sci., Part B: Polym. Phys.* **1987**, *25*, 2497.
(10) Francis, A. W. *J. Phys. Chem.* **1954**, *58*, 1099.
(11) Hoefling, T.; Stofesky, D.; Reid, M.; Beckman, E.; Enick, R. M. *J. Supercrit. Fluids* **1992**, *5*, 237.
(12) McClain, J. B.; DeSimone, J. M. *Science*, in press.
(13) Canelas, D. A.; Betts, D. E.; DeSimone, J. M. *Polym. Mater. Sci. Eng.* **1996**, *74*, 400.
(14) Fulton, J. L.; Pfund, D. M.; McClain, J. B.; Romack, T. J.; Maury, E. E.; Combes, J. R.; Samulski, E. T.; DeSimone, J. M.; Capel, M. *Langmuir* **1995**, *11*, 4241.
(15) McClain, J. B.; Londono, D.; Combes, J. R.; Romack, T. J.; Canelas, D. P.; Betts, D. E.; Wignall, G. D.; Samulski, E. T.; DeSimone, J. M. *J. Am. Chem. Soc.* **1996**, *118*, 917.
(16) McClain, J. B.; Betts, D. E.; Canelas, D. A.; Samulski, E. T.; DeSimone, J. M.; Londono, J. D.; Wignall, G. D. *PMSE Prepr., Am. Chem. Soc., Div. Polym. Mater. Sci. Eng.* **1996**, *74*, 234.
(17) Kazarian, S. G.; Vincent, M. F.; Bright, F. V.; Liotta, C. L.; Eckert, C. A. *J. Am. Chem. Soc.* **1996**, *118*, 1729.
(18) Smith, P. B.; Moll, D. J. *Macromolecules* **1990**, *23*, 3250.
(19) Jonas, J. High Pressure NMR. In *NMR, Basic Principles and Progress*; Diehl, P., Fluck, E., Günther, H., Kosfeld, R., Seelig, J., Eds.; Springer Verlag: Berlin, 1991; Vol. 24.
(20) Yonker, C. R.; Wallen, S. L.; Linehan, J. C. *J. Supercrit. Fluids* **1995**, *8*, 250.
(21) Chen, S.; Miranda, D. T.; Evilia, R. F. *J. Supercrit. Fluids* **1995**, *8*, 255.
(22) DeSimone, J. M.; Guan, Z.; Combes, J. R.; Menceloglu, Y. Z. *Macromolecules* **1993**, *26*, 2663.
(23) Zhang, K.; Cain, J. B.; DeSimone, J. M.; Johnson, C. S. Unpublished data.
(24) March, J. *Advanced Organic Chemistry*; John Wiley & Sons, New York, 1992; p 771.
(25) Guan, Z.; DeSimone, J. M. *Macromolecules* **1994**, *27*, 5527.
(26) Pfund, D. M.; Zemanian, T. S.; Linehan, J. C.; Fulton, J. L.; Yonker, C. R. *J. Phys. Chem.* **1994**, *98*, 11846.
(27) Yonker, C. R.; Zemanian, T. S.; Wallen, S. L.; Linehan, J. C.; Franz, J. A. *J. Magn. Reson., Ser. A* **1995**, *113*, 102.
(28) Dickinson, W. C. *Phys. Rev.* **1951**, *81*, 717.
(29) Buckingham, A. D.; Pople, J. A. *Discyss. Faraday Soc.* **1956**, *22*, 17.
(30) Rummens, F. H. A. Van der Waals Forces and Shielding Effects. In *NMR, Basic Principles and Progress*; Diehl, P., Fluck, H., Kosfeld, R., Seelig, J., Eds.; Springer Verlag: Berlin, 1975; Vol. 10.
(31) *Handbook of Chemistry and Physics*; Chemical Rubber Company: Cleveland, OH, 1968.
(32) Pople, J. A.; Schneider, W. G.; Bernstein, H. J. *High-Resolution Nuclear Magnetic Resonance*; McGraw-Hill: New York, 1959.
(33) Frei, K.; Bernstein, H. J. *J. Chem. Phys.* **1962**, *37*, 1891.
(34) Ely, J. F. *CO_2PAC: A Computer Program to Calculate Physical Properties of Pure CO_2*; National Bureau of Standards: Boulder, CO, 1986.
(35) Cece, A.; Jureller, S. H.; Kerschner, J. L.; Moschner, K. F. *J. Phys. Chem.* **1996**, *100*, 7435.
(36) Lacelle, S.; Cau, F.; Tremblay, L. *J. Phys. Chem.* **1991**, *95*, 7071.
(37) Williams, C.; Brochard, F.; Frisch, H. L. *Annu. Rev. Phys. Chem.* **1981**, *32*, 433.
(38) Doi, M. *Introduction to Polymer Physics*; Clarendon Press: Oxford, England, 1996.
(39) Shultz, A. R.; Flory, P. J. *Macromolecules* **1952**, *74*, 4760.
(40) Wang, W. V.; Kramer, E. J.; Sachse, W. J. *J. Polym. Sci., Polym. Phys. Ed.* **1982**, *20*, 1371.

MA961917E